

Molecular structure and vibrational spectra of 2(5H)-furanone and 2(5H)-thiophenone isolated in low temperature inert matrix

S. Breda, I. Reva *, R. Fausto

Department of Chemistry, University of Coimbra, Rua Larga, 3004-535 Coimbra, Portugal

ARTICLE INFO

Article history:

Received 3 January 2008
Received in revised form 27 February 2008
Accepted 28 February 2008
Available online 8 March 2008

Keywords:

Matrix-isolation
Infrared spectroscopy
2(5H)-Furanone
2(5H)-Thiophenone
MP2 and DFT calculations

ABSTRACT

The structure and vibrational spectra of two five-membered heterocyclic α -carbonyl compounds have been studied. The experimental FTIR spectra 2(5H)-furanone and 2(5H)-thiophenone monomers isolated in inert argon matrices at 10 K are reported and discussed. The interpretation of the experimental data is supported by vibrational calculations at the MP2 and DFT(B3LYP) levels of theory with the 6-311++G(d,p) basis set. Spectra/structure correlations were extracted from the data calculated for the two title compounds and for their six-membered ring analogues, α -pyrone and thiapyran-2-one. The vibrational frequencies of the C=O, CC, CH and CH₂ moieties were correlated with the ring size, atomic charges and the nature of heteroatom. Natural bond orbital analysis revealed important details of the electronic structure and dominant intramolecular interactions in 2(5H)-furanone and 2(5H)-thiophenone and provided an additional insight into their vibrational spectra.

© 2008 Elsevier B.V. All rights reserved.

1. Introduction

2(5H)-Furanone (alternatively also known as γ -crotonolactone or $\Delta^{\alpha\beta}$ -butenolide) is a simplest sub-unit of a large class of five-membered heterocyclic α -carbonyl compounds. The furanone sub-unit is present in a large number of natural products [1–6], which display a wide range of biological activities, and is present in a number of drugs with diverse biological activities, such as antifungal, antibacterial and anti-inflammatory. Recently, it has been shown that 2(5H)-furanone plays an important role in cheese technology [7]. Substituted derivatives of 2(5H)-furanone and its sulphur analogue, 2(5H)-thiophenone, are used in treatment of about 30 most common diseases such as hypertension, infarction, ischemia, arrhythmias, asthmas, atherosclerotic disorders, angina, cancer, stroke and diabetes [8]. A substituted furanone derivative, 3-chloro-4-(dichloromethyl)-5-hydroxy-2(5H)-furanone, also known as Mutagen X, is one of the most potent directing acting mutagens ever tested [9].

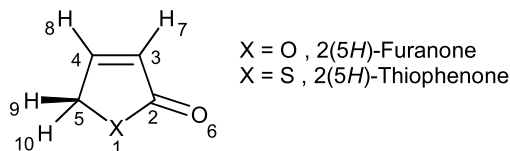
Besides the biological and pharmaceutical importance, 2(5H)-furanone (from here onwards: furanone) and 2(5H)-thiophenone (from here onwards: thiophenone) attract considerable attention as synthetic targets and intermediates [10–14]. Furanone and thiophenone possess an sp³ carbon atom (at position 5, see Scheme 1) that, in the presence of unequal substituents (at positions 9 and 10), affords chirality. Then, furanone and thiophenone are used in

stereoselective synthesis [15,16] to produce chiral compounds and to determine the influences and relative configurations of stereogenic centres [17,18].

A great attention has been dedicated to the issue of planarity of the furanone and thiophenone rings. Theoretical models, considering how the conformation of five-membered ring compounds is controlled by such factors as ring angle strain, torsional forces about ring bonds and substitution of ring atoms, were reported by Legon [19]. Legon et al. also reported experimental studies on the microwave rotational spectrum of furanone [20,21] and showed that its heavy atoms are strictly coplanar at equilibrium. This was concluded based on the measurement of dipole moment components ($\mu_c = 0.0$ D), consideration of the quantity $\Delta_0 = I_c^0 - I_a^0 - I_b^0$ (I^0 standing for the zero-point vibrationally averaged principal moments of inertia), and analysis of the rotational constants and vibrational separations. A similar microwave study was reported by Lesarri et al. for thiophenone [22]. As in the case of furanone, the observed value for $\Delta_0 = I_c^0 - I_a^0 - I_b^0$ and the variation of the rotational constants for thiophenone were also consistent with a planar ring equilibrium configuration.

Vibrational studies of the title compounds are very scarce. Experimental studies using He I and He II photoelectron spectroscopy on furanone [23] and thiophenone [24] revealed in each case two vibrational progressions assigned to skeletal vibrational modes. Very recently, vibrational spectra of liquid (Raman and infrared) and vapour (Raman only) furanone have been reported [25]. The latter study was focused on the planarity of furanone and concluded that it is rigidly planar in the electronic ground

* Corresponding author. Tel.: +351 967 215 641; fax: +351 239 827 703.
E-mail address: reva@qui.uc.pt (I. Reva).



Scheme 1. 2(5H)-Furanone and 2(5H)-thiophenone with atom numbering adopted in this study.

state. To the best of our knowledge, no systematic experimental studies on infrared spectra of monomeric (gaseous or matrix-isolated) furanone and thiophenone have been reported hitherto.

The main objective of the present work was the characterization of the vibrational spectra of monomeric 2(5H)-furanone and 2(5H)-thiophenone.

2. Experimental

Commercial samples of furanone (Aldrich, 98%) and thiophenone (Aldrich, 98%) were used. The chosen compound was placed in a glass ampoule protected against light and connected to the cryostat through a NUPRO SS-4BMRG needle valve with shut-off possibility. Prior to the experiment, the compound was additionally purified from dissolved gases by the multiple freeze – pump – thaw procedure, using the vacuum system of the cryostat. Two parts of the effusive cell, the valve nozzle and the sample compartment, were thermostatted separately. During deposition, the valve nozzle was kept at room temperature, while the sample compartment was cooled to $-50\text{ }^{\circ}\text{C}$ by immersing the ampoule with the compound in a bath with melting sec-Amyl alcohol. This allowed the saturated vapor pressure over the compound to be reduced and the metering function of the valve to be improved. In order to deposit a matrix, the vapour of furanone (or thiophenone) was introduced into the cryostat chamber together with large excess of the host matrix gas (argon N60, Air Liquide) coming from a separate line. Argon was deposited using the standard manometric procedure without further purification. A CsI window was used as optical substrate for the matrices. Its temperature was stabilized at 10 K and measured directly at the sample holder by a silicon diode sensor connected to a digital controller (Scientific Instruments, Model 9650-1), with accuracy of $\pm 0.1\text{ K}$.

The low temperature equipment was based on a closed-cycle helium refrigerator (APD Cryogenics) with a DE-202A expander. The infrared spectra were registered with 0.5 cm^{-1} resolution, in the range $4000\text{--}400\text{ cm}^{-1}$, using a Mattson (Infinity 60AR Series) Fourier transform spectrometer equipped with a deuterated triglycine sulphate (DTGS) detector and a KBr beamsplitter. The sample compartment of the spectrometer was modified in order to couple it with the cryostat head and allow purging of the instrument by a stream of dry nitrogen to remove water vapour and CO_2 .

3. Computational details

The equilibrium geometries of the studied species were fully optimized at the DFT and MP2 levels of theory with the standard 6-311++G(d,p) basis set and are collected in Table S1 (Supplementary material). The DFT calculations were carried out with the three-parameter density functional abbreviated as B3LYP, which includes Becke's gradient exchange correction [26], the Lee, Yang, Parr correlation functional [27] and the Vosko, Wilk and Nusair correlation functional [28]. No symmetry restrictions were imposed to the initial structures; however, both furanone and thiophenone rings converged to the planar structures. After-

Table 1

Internal coordinates used in the normal modes analyses for 2(5H)-furanone (X=O) and 2(5H)-thiophenone (X=S)^a

$S_1 = r_{1,2}$	$\nu(\text{X1-C2})$
$S_2 = r_{2,3}$	$\nu(\text{C2-C3})$
$S_3 = r_{3,4}$	$\nu(\text{C3=C4})$
$S_4 = r_{4,5}$	$\nu(\text{C4-C5})$
$S_5 = r_{5,1}$	$\nu(\text{C5-X1})$
$S_6 = r_{2,6}$	$\nu(\text{C2=O6})$
$S_7 = r_{3,7}$	$\nu(\text{C3-H7})$
$S_8 = r_{4,8}$	$\nu(\text{C4-H8})$
$S_9 = (2^{-1/2})(r_{5,9} + r_{5,10})$	$\nu(\text{CH}_2)_s$
$S_{10} = (2^{-1/2})(r_{5,9} - r_{5,10})$	$\nu(\text{CH}_2)_a$
$S_{11} = (1 + 2a^2 + 2b^2)^{-1/2} [\beta_{5,2,1} + a(\beta_{1,3,2} + \beta_{1,4,5}) + b(\beta_{2,4,3} + \beta_{3,5,4})]$	$\delta\text{ ring 1}$
$S_{12} = 1/2[(a-b)^2 + (1-a)^2]^{-1/2} [(a-b)(\beta_{1,3,2} - \beta_{1,4,5}) + (1-a)(\beta_{2,4,3} - \beta_{3,5,4})]$	$\delta\text{ ring 2}$
$S_{13} = (2^{-1/2})(\beta_{6,1,2} - \beta_{6,3,2})$	$\delta(\text{C2=O6})$
$S_{14} = (2^{-1/2})(\beta_{7,2,3} - \beta_{7,4,3})$	$\delta(\text{C3-H7})$
$S_{15} = (2^{-1/2})(\beta_{8,3,4} - \beta_{8,5,4})$	$\delta(\text{C4-H8})$
$S_{16} = (20^{-1/2})(4\beta_{10,9,5} - \beta_{10,1,5} - \beta_{9,1,5} - \beta_{10,4,5} - \beta_{9,4,5})$	$\delta(\text{CH}_2)\text{scis}$
$S_{17} = (1/2)(\beta_{10,1,5} + \beta_{9,1,5} - \beta_{10,4,5} - \beta_{9,4,5})$	$\delta(\text{CH}_2)\text{wag}$
$S_{18} = (1/2)(\beta_{10,1,5} - \beta_{9,1,5} - \beta_{10,4,5} + \beta_{9,4,5})$	$\delta(\text{CH}_2)\text{twist}$
$S_{19} = (1/2)(\beta_{10,1,5} - \beta_{9,1,5} + \beta_{10,4,5} - \beta_{9,4,5})$	$\delta(\text{CH}_2)\text{rock}$
$S_{20} = (2b^2 + 2a^2 + 1)^{-1/2} [b(\tau_{5,1,2,3} + \tau_{4,5,1,2}) + a(\tau_{1,2,3,4} - \tau_{3,4,5,1}) + \tau_{2,3,4,5}]$	$\tau\text{ ring 1}$
$S_{21} = 1/2[(a-b)^2 + (1-a)^2]^{-1/2} [(a-b)(\tau_{3,4,5,1} - \tau_{1,2,3,4}) + (1-a)(\tau_{4,5,1,2} - \tau_{5,1,2,3})]$	$\tau\text{ ring 2}$
$S_{22} = \gamma_{6,1,2,3}$	$\gamma(\text{C2=O6})$
$S_{23} = \gamma_{7,2,3,4}$	$\gamma(\text{C3-H7})$
$S_{24} = \gamma_{8,3,4,5}$	$\gamma(\text{C4-H8})$

$r_{i,j}$ is the distance between atoms A_i and A_j ; $\beta_{i,j,k}$ is the angle between vectors A_kA_i and A_kA_j ; $\tau_{i,j,k,l}$ is the dihedral angle between the plane defined by A_i, A_j, A_k and the plane defined by A_j, A_k, A_l atoms; $\gamma_{i,j,k,l}$ is the angle between the vector A_kA_i and the plane defined by atoms A_j, A_k, A_l ; $a = \cos 144^\circ$, $b = \cos 72^\circ$.

^a Atom numbering as in Scheme 1.

wards, geometry optimizations and calculations of harmonic frequencies were carried out using explicit C_s symmetry. The nature of the obtained stationary points was checked through the analysis of the corresponding Hessian matrices. For the planar structures, no imaginary frequencies were obtained, indicating that they correspond to true minima. A set of internal coordinates was defined and the Cartesian force constants were transformed to the internal coordinate space, allowing ordinary normal-coordinate analysis to be performed as described by Schachtschneider and Mortimer [29]. The calculated harmonic frequencies were also used to assist the analysis of the experimental spectra. Internal coordinate sets defined for furanone and thiophenone are given in Table 1. All calculations in this work were done using the Gaussian 03 program [30]. To better understand the specific nature of the intramolecular interactions in the studied compounds, their electronic structures were characterized by Natural Bond Orbital (NBO) analysis, using NBO version 3, as implemented in Gaussian 03.

4. Results and discussion

4.1. Analysis of the vibrational spectra of furanone and thiophenone

4.1.1. Choice of appropriate scaling factors for calculated frequencies

Along this article, a detailed comparison between the observed infrared spectra of furanone and thiophenone and their theoretically predicted spectra obtained both at the MP2 and DFT levels of theory is presented. As usually, the obtained theoretical frequencies systematically overestimate the experimental ones, mainly due to the non-consideration of anharmonicity in the theoretical treatment and also due to basis set limitations and incomplete consideration of electron correlation. In order to facilitate the comparison, the calculated frequencies were then subjected to scaling. The choice of scaling factors applied to the calculated frequencies has

been accomplished in the following steps. In a first step, the studied compound was trapped in a low temperature inert matrix and the experimental infrared spectrum of the isolated compound was obtained. In the second step, the calculated spectrum of the monomer in vacuum was subjected to linear fit against the experimental data. For both compounds, the fourteen most intense experimental bands in the fingerprint region of the spectrum ($1900\text{--}500\text{ cm}^{-1}$) were used in this procedure. The least squares linear regression through the origin of coordinates resulted in the following scaling coefficients: 0.9834 (DFT) and 0.9768 (MP2) for furanone, 0.9764 (DFT) and 0.9736 (MP2) for thiophenone, with correlation coefficients equal to 0.9997, 0.9996, 0.9994 and 0.9986, respectively. In the third step, the individual scaling factors for the same theory level were defined as the average of those obtained for the two compounds, i.e. 0.980 (DFT) and 0.975 (MP2) (rounded to the third significant digit). These averaged scaling factors were used throughout the present study.

4.1.2. Assignment of the spectra of the matrix-isolated compounds

The most intense feature in the infrared spectra of both furanone and thiophenone is due to the carbonyl stretching vibration. For each compound, there is only one vibration in this spectral region predicted by harmonic calculations. However, in the experimental spectra of the matrix-isolated compounds, several satellite bands of weaker intensity accompany the main peak, the multiplets spanning over tens of reciprocal centimeters (Fig. 1).

In furanone and other common unsaturated five- and six-membered ring lactones in solution [31,32] the carbonyl absorption band was found to exhibit a doublet structure. Jones et al. [32] interpreted this phenomenon in terms of Fermi-resonance interactions between the carbonyl stretching vibration and overtones or

combinations of low-frequency fundamentals. It appears that such splitting of the C=O stretching absorption band occurs not only in solution but also for matrix-isolated lactones. Indeed, besides furanone and thiophenone (see Fig. 1), we have also observed previously similar Fermi-resonance splitting for other monocyclic lactones isolated in cryogenic inert matrices, in particular for α -pyrone [33] and thiapyran-2-one [34], which are six-membered ring lactones closely related structurally with furanone and thiophenone. Splitting of the C=O stretching absorption was also observed for a series of differently substituted α -pyrones [35,36] and for the bicyclic lactone coumarin (2-benzopyrone) [37]. Moreover, a strong Fermi-resonance splitting of the C=O stretching bands was also experimentally observed for matrix-isolated uracil [38].

It should be noted here that the carbonyl stretching vibration appears at lower frequency in thiophenone than in furanone. The separation in these frequencies predicted by the MP2 method (86.7 cm^{-1}) is closer to the experimental value (79.5 cm^{-1}) than that obtained by the DFT method (61.6 cm^{-1}).

The comparison of the two experimental spectra in the carbonyl stretching region shows also that in the spectrum of matrix-isolated thiophenone a weak absorption at 1793.5 cm^{-1} , i.e. at the same frequency where furanone absorbs, is observed. This suggests the presence in the thiophenone sample of residual traces of furanone. However, because both compounds are well-isolated in the matrix, furanone monomers do not interfere with thiophenone monomers and do not constitute any source of problems in relation with the present study.

The fingerprint region of the experimental FTIR spectrum of matrix-isolated furanone is shown in Fig. 2, where it is compared with the theoretical spectrum of the monomer calculated at two different theory levels. The spectral assignments are summarized in Table 2. There is a good overall agreement between the experimental and calculated frequencies and the assignment of the most intense bands is straightforward. The scissoring, wagging, twisting and rocking modes of the CH_2 group are well localized and appear at 1454.4 , 1343.6 , 1164.9 and 1008.3 cm^{-1} , respectively.

The three intense bands that dominate the infrared spectrum of furanone between 1150 and 1040 cm^{-1} originate in A' symmetry bending vibrations mainly localized in the two C–H groups and the two ring C–O bonds (with different phase combinations). The relative frequencies of these three bands are well predicted by both DFT and MP2 methods, while none of them could correctly predict the relative intensities. The failure in prediction of correct relative intensities is probably due to highly-mixed contributions of different coordinates to these normal modes, since small variations in PEDs (see Table 2) can strongly affect the magnitudes of the dipole moment derivatives.

There are three modes appearing between 900 and 750 cm^{-1} that deserve a special comment. The strong band at 866.5 cm^{-1} (A') is due to mixed O1–C2 and C2–C3 stretching vibrations, with the O–C component dominating. The next strong band, at 804.9 cm^{-1} (A''), is assigned to the out-of-plane vibration of the carbonyl group (ca. 50% PED contribution), with additional contributions from the out-of-plane vibrations of the two C–H groups (ca. 20% each). Finally, the weak band at 783.2 cm^{-1} (A') is due to a ring deformation vibration. The intensities of these three bands are well predicted by both MP2 and DFT calculations (which are also mutually consistent regarding predicted PEDs), while the relative frequencies are clearly better predicted by the DFT method (Table 2). The assignments in this spectral region seem to us unequivocal, though Al-Saadi and Laane [25] have assigned the carbonyl out-of-plane and the ring bending modes (ν_{21} and ν_{14} in their notation) in the opposite way.

On the other hand, in the region between 970 and 910 cm^{-1} the assignments were not so easy to do. There are two vibrations

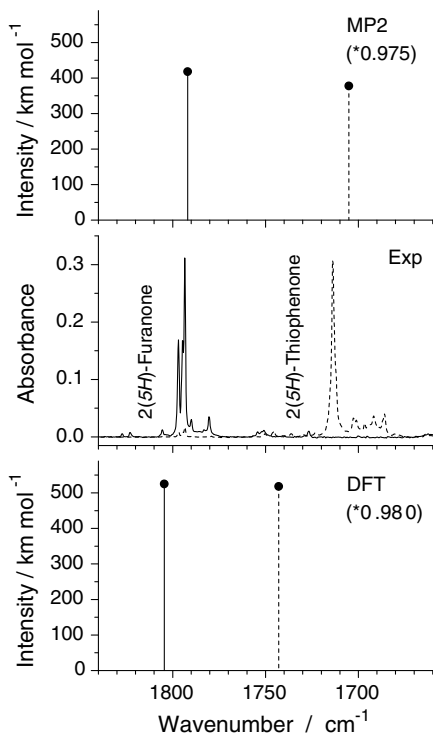


Fig. 1. Region of the carbonyl stretching vibration in the experimental FTIR spectra of 2(5H)-furanone (solid line) and 2(5H)-thiophenone (dashed line) isolated in argon matrices at 10 K (middle frame). The theoretical spectra of the corresponding monomers (solid lines, furanone; dashed lines, thiophenone) were calculated at the DFT(B3LYP)/6-311++G(d,p) (bottom frame) and MP2/6-311++G(d,p) (top frame) levels of theory. The calculated frequencies were scaled by the factors of 0.980 (DFT) and 0.975 (MP2).

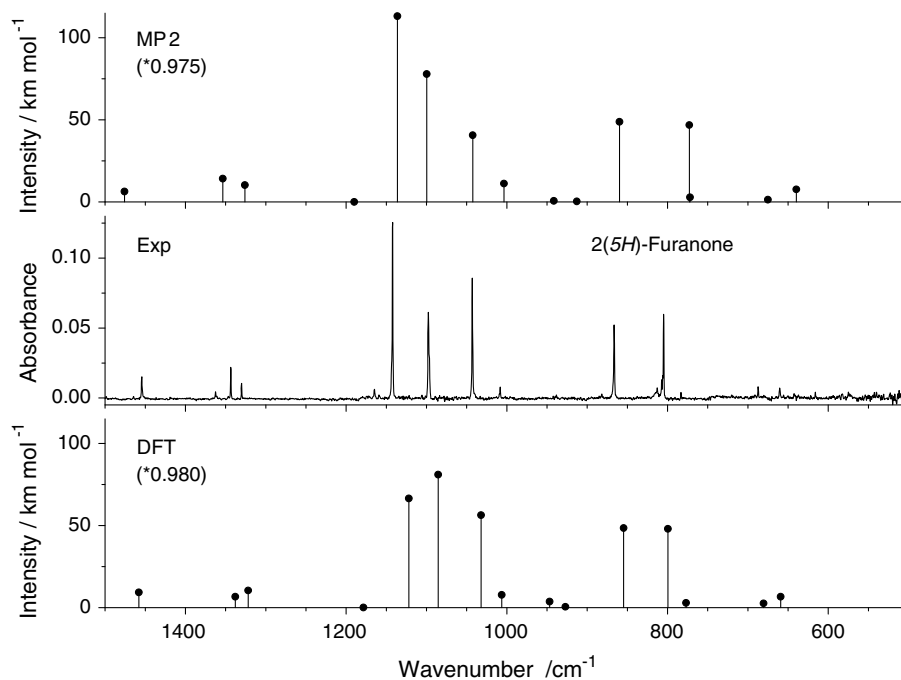


Fig. 2. Fingerprint region of the experimental FTIR spectrum of 2(5H)-furanone isolated in an argon matrix at 10 K (middle frame) compared to the theoretical spectra of the monomer calculated at the DFT(B3LYP)/6-311++G(d,p) (bottom frame) and MP2/6-311++G(d,p) (top frame) levels of theory. The calculated frequencies were scaled by the factors of 0.980 and 0.975, respectively.

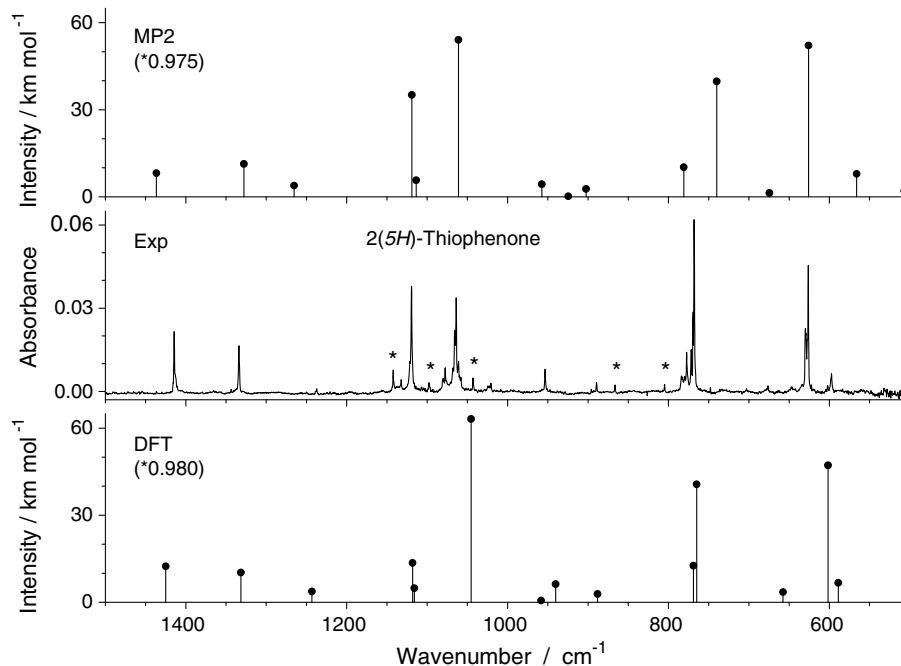


Fig. 3. Fingerprint region of the experimental FTIR spectrum of 2(5H)-thiophenone isolated in an argon matrix at 10 K (middle frame) compared to the theoretical spectra of the monomer calculated at the DFT(B3LYP)/6-311++G(d,p) (bottom frame) and MP2/6-311++G(d,p) (top frame) levels of theory. The calculated frequencies were scaled by the factors of 0.980 and 0.975, respectively. Asterisks indicate the bands due to 2(5H)-furanone trace impurity.

predicted to give rise to bands of very weak infrared intensity in this region, one with dominant contribution of the out-of-plane C3–H7 coordinate (A'') and the other with major contribution from the C4–C5 stretching coordinate (A'). The relative frequencies of these two vibrations are predicted in the opposite order by the DFT and MP2 calculations (see Table 2). The assignment of these

two modes by Al-Saadi and Laane [25], based on the experimental Raman spectra (where the A' mode appears as an intense band), validates the order of frequencies predicted by the DFT calculations.

The fingerprint region of the experimental FTIR spectrum of matrix-isolated thiophenone is shown in Fig. 3. Like in the carbonyl

Table 2

Experimentally observed FTIR spectrum (argon matrix, $T = 10$ K), Raman (vapour) and theoretical vibrational frequencies (ω , cm^{-1}), infrared intensities (I , km mol^{-1}) and potential energy distributions (PED) for 2(5H)-furanone monomer calculated at the B3LYP/6-311++G(d,p) and MP2/6-311++G(d,p) levels of theory

Observed (Ar, $T = 10$ K)		Raman Ref. [25]				Calculated B3LYP/6-311++G(d, p)				Calculated MP2/6-311++G(d, p)		
ω	A^a	ω	I	ω^b	I	Sym.	PED ^d (%)	ω^c	I	PED ^d (%)		
		3123	(47)	3183.9	0.3	A'	$\nu(\text{C3-H7})(91.0)$	3208.3	0.3	$\nu(\text{C3-H7})(88.6) + \nu(\text{C4-H8})(10.2)$		
		3097	(80)	3145.6	1.7	A'	$\nu(\text{C4-H8})(91.4)$	3171.9	0.7	$\nu(\text{C4-H8})(89.0) + \nu(\text{C3-H7})(10.5)$		
2935.1	5.5	2947	(134)	3003.2	10.3	A''	$\nu(\text{CH}_2)\text{as}(100.0)$	3065.2	8.3	$\nu(\text{CH}_2)\text{as}(100.0)$		
2877.9	7.9	2885	(233)	2972.1	20.3	A'	$\nu(\text{CH}_2)\text{s}(100.0)$	3014.9	19.5	$\nu(\text{CH}_2)\text{s}(100.0)$		
1796.8, 1793.5 ^e	479.2	1809	(100)	1804.5	525.2	A'	$\nu(\text{C2=O6})(87.9)$	1791.9	418.3	$\nu(\text{C2=O6})(86.3)$		
1610.8	3.1	1609	(77)	1621.3	8.1	A'	$\nu(\text{C3=C4})(82.2)$	1603.3	1.3	$\nu(\text{C3=C4})(81.2)$		
1454.4	15.2	1462	(46)	1457.9	9.3	A'	$\delta(\text{CH}_2)\text{scis}(97.6)$	1475.7	6.3	$\delta(\text{CH}_2)\text{scis}(97.2)$		
1362.6	4.8											
1343.6	18.1	1358	(5)	1338.0	6.7	A'	$\delta(\text{CH}_2)\text{wag}(69.5) + \nu(\text{C4-C5})(13.1)$	1353.4	14.2	$\delta(\text{CH}_2)\text{wag}(75.7) + \nu(\text{C4-C5})(10.5)$		
1330.3	8.0	1328	(8)	1322.0	10.5	A'	$\delta(\text{C4-H8})(36.1) + \delta(\text{C3-H7})(25.9) + \nu(\text{C2-C3})(12.8) + \delta(\text{CH}_2)\text{wag}(10.2)$	1326.0	10.3	$\delta(\text{C4-H8})(37.0) + \delta(\text{C3-H7})(27.6) + \nu(\text{C2-C3})(14.4)$		
1164.9, 1159.0	11.2	1153	(8)	1178.4	0.1	A''	$\delta(\text{CH}_2)\text{twist}(88.4) + \delta(\text{CH}_2)\text{rock}(10.0)$	1189.8	0.03	$\delta(\text{CH}_2)\text{twist}(86.5) + \delta(\text{CH}_2)\text{rock}(12.5)$		
1142.2	103.3	1140	(19)	1122.0	66.6	A'	$\delta(\text{C3-H7})(30.6) + \nu(\text{C2-C3})(19.4) + \delta(\text{C2=O6})(17.7) + \nu(\text{O1-C2})(12.9)$	1136.2	113.2	$\delta(\text{C3-H7})(22.2) + \nu(\text{C2-C3})(21.0) + \delta(\text{C2=O6})(16.6) + \nu(\text{O1-C2})(21.2) + \delta(\text{CH}_2)\text{wag}(11.1)$		
1097.6	73.4	1095	(25)	1085.4	81.1	A'	$\delta(\text{C4-H8})(34.0) + \nu(\text{C5-O1})(19.2) + \delta(\text{C3-H7})(11.7) + \delta$ ring 2(12.0) + $\nu(\text{O1-C2})(10.7)$	1099.6	77.9	$\delta(\text{C4-H8})(23.8) + \nu(\text{C5-O1})(43.6) + \delta(\text{C3-H7})(12.8)$		
1043.1	70.3	1043	(37)	1032.1	56.4	A'	$\nu(\text{C5-O1})(46.4) + \delta(\text{C3-H7})(14.8) + \nu(\text{C4-C5})(10.9)$	1042.3	40.7	$\nu(\text{C5-O1})(27.0) + \delta(\text{C3-H7})(24.5) + \nu(\text{C4-C5})(9.9) + \delta(\text{C4-H8})(15.7)$		
1008.3	6.8	998	(1)	1006.3	7.8	A''	$\delta(\text{CH}_2)\text{rock}(62.8) + \gamma(\text{C4-H8})(29.3)$	1003.5	11.2	$\delta(\text{CH}_2)\text{rock}(72.3) + \gamma(\text{C4-H8})(13.3)$		
938.4 ^f	4.3	973	(4)	946.6	3.7	A''	$\gamma(\text{C3-H7})(65.1) + \gamma(\text{C4-H8})(29.3) + \delta(\text{CH}_2)\text{rock}(10.6)$	913.0	0.4	$\gamma(\text{C3-H7})(61.9) + \gamma(\text{C4-H8})(47.5)$		
938.4 ^f		939	(40)	927.1	0.5	A'	$\nu(\text{C4-C5})(64.8) + \nu(\text{C5-O1})(12.8) + \delta(\text{C4-H8})(11.0)$	941.4	0.6	$\nu(\text{C4-C5})(61.8) + \nu(\text{C5-O1})(13.5) + \delta(\text{C4-H8})(13.9)$		
881.6	1.9											
866.5	49.2	865	(45)	854.7	48.5	A'	$\nu(\text{O1-C2})(49.2) + \nu(\text{C2-C3})(25.5)$	859.7	48.8	$\nu(\text{O1-C2})(46.9) + \nu(\text{C2-C3})(27.3)$		
813.0	2.5											
804.9	51.0	830	(4)	799.5	48.0	A''	$\gamma(\text{C2=O6})(49.7) + \gamma(\text{C3-H7})(18.0) + \gamma(\text{C4-H8})(20.7) + \tau$ ring 1(10.4)	772.9	46.8	$\gamma(\text{C2=O6})(49.8) + \gamma(\text{C3-H7})(25.0) + \gamma(\text{C4-H8})(17.2)$		
783.2	3.7	804	(9)	776.9	2.9	A'	δ ring 2(43.1) + δ ring 1(28.1) + $\nu(\text{C2-C3})(15.8)$	771.9	2.8	δ ring 2(46.7) + δ ring 1(29.1) + $\nu(\text{C2-C3})(13.3)$		
687.2	3.7	683	(55)	680.5	2.6	A'	δ ring 1(46.7) + δ ring 2(20.6)	675.1	1.4	δ ring 1(46.8) + δ ring 2(22.4)		
660.4	6.8	663	(5)	659.3	6.7	A''	$\gamma(\text{C2=O6})(31.0) + \gamma(\text{C4-H8})(23.8) + \gamma(\text{C3-H7})(20.5)$	639.7	7.6	$\gamma(\text{C2=O6})(33.8) + \gamma(\text{C4-H8})(26.4) + \gamma(\text{C3-H7})(17.7)$		
616.0	3.7											
n.i.		490	(8)	485.6	2.3	A'	$\delta(\text{C2=O6})(72.2) + \nu(\text{C2-C3})(10.8)$	482.3	2.3	$\delta(\text{C2=O6})(73.7) + \nu(\text{C2-C3})(9.9)$		
n.i.		~366	(0)	342.4	6.6	A''	τ ring 1(78.2) + τ ring 2(15.3)	310.0	6.0	τ ring 1(84.2) + τ ring 2(11.5)		
n.i.		208	(1)	199.1	0.5	A''	τ ring 2(76.9) + $\gamma(\text{C2=O6})(12.0) + \tau$ ring 1(10.9)	182.1	0.9	τ ring 2(82.2)		

Definition of symmetry coordinates is given in Table 1. See Scheme 1 for atom numbering. Abbreviations: s, symmetric; as, antisymmetric; scis, scissoring; wag, wagging; twist, twisting; rock, rocking; ν , stretching; δ , in-plane bending; γ , out-of-plane bending; τ , torsion; n.i., not investigated.

^a Relative integrated intensities.

^b Theoretical frequencies calculated at the DFT(B3LYP)/6-311++G(d,p) level were scaled by a factor of 0.980.

^c Theoretical frequencies calculated at the MP2/6-311++G(d,p) level were scaled by a factor of 0.975.

^d PED's lower than 10% are not included.

^e The C=O stretching vibration is strongly anharmonic and has many satellite bands. In the table only the main peak is indicated. The satellite bands appear at the following frequencies: 1925.5 (11.2); 1827.2 (3.7); 1823.0 (6.8); 1805.5 (11.8); 1780.3 (33.6); 1751.2 (36.7); 1726.7 (12.4) (relative intensities in parentheses).

^f Assignment unclear.

stretching region, there are also a few weak absorptions in the fingerprint region of the experimental spectrum that are not predicted by the calculations. These extra bands (marked by asterisks in Fig. 3) are due to absorptions of furanone monomers present in the matrix as vestigial impurity (compare with Fig. 2). The remaining bands in the experimental spectrum are doubtlessly ascribable to thiophenone. The corresponding spectral assignments are summarized in Table 3.

As in the case of furanone, the scissoring, wagging, twisting and rocking modes of the CH_2 group are also well localized and appear at 1414.6, 1237.1, 1119.5 and 889.6 cm^{-1} , respectively. It should be however noted, that these modes are strongly shifted to lower frequencies upon substitution of the ring oxygen by sulphur. The MP2 calculated reduced masses and force constants (Dalton; $\text{mDyn } \text{\AA}^{-1}$, respectively) for these modes are: (1.091; 1.473), (1.630; 1.851), (1.083; 0.950) and (1.694; 1.057), for furanone, and (1.091; 1.395), (1.552; 1.540), (1.087; 0.835) and (1.463; 0.738), for thiophenone, which clearly reveals that the smaller frequencies observed for thiophenone result from substantially smaller force constants associated with the

CH_2 bending vibrations in this molecule than in furanone. This, in turn, might be correlated with the charge on the C5 atom, which is significantly more negative in thiophenone than in furanone. In furanone, the ring oxygen atom, bound to C5, is a strong electron attractor and therefore polarizes more the C–H bonds in the methylene group reducing the electron density (and hence the force constants) in these bonds. Note that in agreement with this explanation, the calculated frequencies for the CH_2 stretching modes are also considerably lower in thiophenone than in furanone (see Tables 2 and 3).

Another interesting consequence on the molecular vibrations of the substitution of the ring oxygen by the heavier sulphur is that the in-plane vibrations of the two C–H groups are not any more mixed with the vibrations of the polar C–O ring bonds. Because of this, the uncoupled C–H bending vibrations of thiophenone lose infrared intensity (comparing to the similar modes of furanone) and appear at 1334.1 and 1119.5 cm^{-1} . On the other hand, the third normal mode with significant C–H in-plane bending contribution in thiophenone corresponds to a vibration where the C4–H8 bending coordinate is strongly mixed with the C–C

Table 3
Experimentally observed FTIR spectrum (argon matrix, $T = 10$ K) and theoretical vibrational frequencies (ω , cm^{-1}), infrared intensities (I , km mol^{-1}) and potential energy distributions (PED) for 2(5H)-thiophenone monomer calculated at the B3LYP/6-311++G(d,p) and MP2/6-311++G(d,p) levels of theory

Observed (Ar, $T = 10$ K)		Calculated B3LYP/6-311++G(d, p)				Calculated MP2/6-311++G(d, p)		
ω	A^a	ω^b	I	Sym.	PED ^d (%)	ω^c	I	PED ^d (%)
		3149.1	1.4	A'	$\nu(\text{C3-H7})(89.4) + \nu(\text{C4-H8})(9.7)$	3175.6	0.8	$\nu(\text{C3-H7})(88.1) + \nu(\text{C4-H8})(10.9)$
		3115.6	2.3	A'	$\nu(\text{C4-H8})(89.7) + \nu(\text{C3-H7})(10.0)$	3141.4	1.5	$\nu(\text{C4-H8})(88.4) + \nu(\text{C3-H7})(11.2)$
		3019.2	1.4	A''	$\nu(\text{CH}_2)\text{as}(100.0)$	3067.3	0.7	$\nu(\text{CH}_2)\text{as}(100.0)$
2926.4	2.3	2983.7	8.8	A'	$\nu(\text{CH}_2)\text{s}(100.0)$	3015.7	7.2	$\nu(\text{CH}_2)\text{s}(100.0)$
1713.9 ^e	420.8	1742.9	518.1	A'	$\nu(\text{C2=O})(92.4)$	1705.2	377.7	$\nu(\text{C2=O})(90.2)$
1615.4	2.5	1629.1	12.6	A'	$\nu(\text{C3=C4})(80.5)$	1608.4	1.2	$\nu(\text{C3=C4})(79.2)$
1414.6	22.3	1424.9	12.4	A'	$\delta(\text{CH}_2)\text{scis}(98.5)$	1436.6	8.2	$\delta(\text{CH}_2)\text{scis}(98.9)$
1334.1	14.2	1331.6	10.3	A'	$\delta(\text{C4-H8})(44.5) + \delta(\text{C3-H7})(33.6)$	1327.7	11.3	$\delta(\text{C4-H8})(43.6) + \delta(\text{C3-H7})(30.9) + \nu(\text{C2-C3})(10.7)$
1237.1	1.7	1243.3	3.7	A'	$\delta(\text{CH}_2)\text{wag}(76.6) + \nu(\text{C4-C5})(11.0)$	1265.4	3.9	$\delta(\text{CH}_2)\text{wag}(77.1) + \nu(\text{C4-C5})(12.3)$
1132.2	1.8							
1119.5 ^f	47.3	1118.0	13.6	A'	$\delta(\text{C3-H7})(51.1) + \delta(\text{C4-H8})(19.9) + (\text{CH}_2)\text{wag}(10.2)$	1119.0	35.1	$\delta(\text{C3-H7})(48.6) + \delta(\text{C4-H8})(9.6) + \nu(\text{C2-C3})(15.7)$
1119.5 ^f		1115.8	4.9	A''	$\delta(\text{CH}_2)\text{twist}(88.6)$	1113.7	5.7	$\delta(\text{CH}_2)\text{twist}(94.1)$
1080.1	2.3							
1077.6	2.9							
1063.8	64.0	1045.4	63.2	A'	$\nu(\text{C2-C3})(38.5) + \delta(\text{C4-H8})(22.7) + \delta \text{ ring } 2(15.1) + \delta(\text{C2=O})(14.8)$	1061.1	54.1	$\nu(\text{C2-C3})(27.2) + \delta(\text{C4-H8})(34.8) + \delta \text{ ring } 2(10.7) + \delta(\text{C2=O})(10.3)$
1020.8	1.2							
		958.2	0.6	A''	$\gamma(\text{C3-H7})(56.0) + \gamma(\text{C4-H8})(53.5)$	924.6	0.2	$\gamma(\text{C3-H7})(54.7) + \gamma(\text{C4-H8})(55.8)$
953.4	5.3	940.2	6.3	A'	$\nu(\text{C4-C5})(71.6) + \delta(\text{CH}_2)\text{wag}(10.4)$	957.5	4.4	$\nu(\text{C4-C5})(67.9) + \delta(\text{CH}_2)\text{wag}(10.4.5)$
889.6	2.5	888.3	2.9	A''	$\delta(\text{CH}_2)\text{rock}(70.9) + \gamma(\text{C3-H7})(15.0)$	902.3	2.7	$\delta(\text{CH}_2)\text{rock}(75.9) + \gamma(\text{C3-H7})(15.1)$
783.8, 777.5	26.9	769.1	12.6	A'	$\delta \text{ ring } 2(54.3) + \nu(\text{C5-S1})(22.4) + \nu(\text{C2-C3})(11.2)$	781.0	10.2	$\delta \text{ ring } 2(41.3) + \nu(\text{C5-S1})(38.3)$
771.7, 768.1	68.9	764.9	40.7	A''	$\gamma(\text{C4-H8})(30.0) + \gamma(\text{C2=O})(28.9) + \gamma(\text{C3-H7})(26.2)$	740.0	39.8	$\gamma(\text{C4-H8})(33.1) + \gamma(\text{C2=O})(27.4) + \gamma(\text{C3-H7})(29.4)$
747.7	1.0							
		657.5	3.5	A'	$\nu(\text{C5-S1})(56.6) + \delta \text{ ring } 2(13.9) + \nu(\text{C2-C3})(15.1)$	674.6	1.3	$\nu(\text{C5-S1})(44.6) + \delta \text{ ring } 2(26.9) + \nu(\text{C2-C3})(17.4)$
629.8, 626.3	60.0	601.7	47.2	A'	$\nu(\text{S1-C2})(45.5) + \delta(\text{C2=O})(21.3) + \nu(\text{C5-S1})(12.2)$	625.8	52.1	$\nu(\text{S1-C2})(52.8) + \delta(\text{C2=O})(15.4) + \nu(\text{C2-C3})(9.6) + \delta \text{ ring } 2(9.6)$
597.3	6.4	588.9	6.7	A''	$\gamma(\text{C2=O})(51.7) + \gamma(\text{C4-H8})(10.9) + \tau \text{ ring } 1(12.3) + \delta(\text{CH}_2)\text{rock}(11.6)$	566.0	7.9	$\gamma(\text{C2=O})(55.5) + \gamma(\text{C4-H8})(12.6) + \tau \text{ ring } 1(11.7)$
		501.5	2.3	A'	$\delta \text{ ring } 1(84.0)$	506.8	2.0	$\delta \text{ ring } 1(84.4)$
n.i.		388.8	4.3	A'	$\delta(\text{C2=O})(50.8) + \nu(\text{S1-C2})(41.9)$	403.1	3.6	$\delta(\text{C2=O})(58.1) + \nu(\text{S1-C2})(32.3)$
n.i.		321.2	2.4	A''	$\tau \text{ ring } 1(83.8) + \gamma(\text{C2=O})(15.0)$	292.4	2.3	$\tau \text{ ring } 1(88.0) + \gamma(\text{C2=O})(14.3)$
n.i.		150.4	0.001	A''	$\tau \text{ ring } 2(92.8)$	134.0	0.0002	$\tau \text{ ring } 2(95.5)$

Definition of symmetry coordinates is given in Table 1. See Scheme 1 for atom numbering. Abbreviations: s, symmetric; as, antisymmetric; scis, scissoring; wag, wagging; twist, twisting; rock, rocking; ν , stretching; δ , in-plane bending; γ , out-of-plane bending; τ , torsion; n.i., not investigated.

A small amount of 2(5H)-furanone (as impurity) was found in the sample of matrix-isolated 2(5H)-thiophenone. The six furanone bands with the strongest infrared absorption have the following experimental frequencies (relative intensities in parentheses): 1796.8/1793.3 (22.3); 1142.1 (5.1); 1097.5 (3.7); 1042.9 (3.1); 866.4 (2.2); 804.9 (1.5). These bands are designated by asterisks in Fig. 3 and assigned in Table 2.

^a Relative integrated intensities.

^b Theoretical frequencies calculated at the DFT(B3LYP)/6-311++G(d,p) level were scaled by a factor 0.980.

^c Theoretical frequencies calculated at the MP2/6-311++G(d,p) level were scaled by a factor 0.975.

^d PED's lower than 10% are not included.

^e The C=O stretching vibration is strongly anharmonic and has many satellite bands. In the table only the main peak is indicated. The satellite bands appear at the following frequencies: 1750.0 (6.5); 1745.3 (9.6); 1736.0 (4.0); 1729.8 (3.7); 1723.2 (3.4); 1702.8/1701.3 (34.0); 1696.7 (6.5); 1691.8 (28.1); 1685.2 (27.5); 1664.3 (3.4) (relative intensities in parentheses).

^f Two theoretically predicted modes assigned to the same absorption in the experiment.

stretching, C=O bending and a ring bending coordinate and is ascribable to the infrared band observed at 1063.8 cm^{-1} , whose intensity remains strong.

Some trends found in the vibrational calculations of furanone persisted in the calculations of thiophenone. For example, most of the vibrations in the region from 1000 to 500 cm^{-1} exhibit a strong coupling between different coordinates. In addition, like in furanone, the theoretical DFT and MP2 calculations were unable to agree in the relative order of the two vibrational modes predicted to occur between 970 and 910 cm^{-1} (C–H out-of-plane (A'') and C4–C5 stretching (A') modes). Furthermore, also like for furanone, the overall relative frequencies of thiophenone computed by the DFT method were found to be in a better agreement with the experiment than those obtained at the MP2 level of theory.

4.2. Comparative analysis of structures of furanone and thiophenone

4.2.1. Spectra-structure correlations

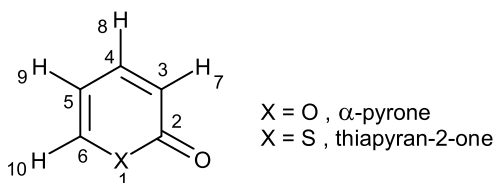
It is interesting to follow the behaviour of the carbonyl stretching frequency in heterocyclic α -carbonyl compounds as a function

of the ring size. Nyquist et al. reported [39] that, when the amount of ring strain decreases (i.e. the ring size increases), the carbonyl stretching frequency also decreases. In addition, it was also observed that conjugation of the C=O group with the C=C bonds of unsaturated rings results in lowering of the C=O stretching frequency in comparison with those of saturated rings of the same size. These trends were observed, for example, for β -propiolactone, γ -butyrolactone, furanone and α -pyrone in CCl_4 and CHCl_3 solutions [39]. The experimental data for matrix-isolated furanone (five-membered lactone) and the literature data on lactones of different ring sizes fit well into this scheme. The carbonyl stretching frequency decreases in the following series, where the ring strain progressively decreases: 1906 cm^{-1} for gaseous cyclopropanone [40], 1815 cm^{-1} for gaseous cyclobutanone [40], 1793.5 cm^{-1} for matrix-isolated furanone (present study), and 1757 cm^{-1} for matrix-isolated α -pyrone [33].

Recently, Bach and Dmitrenko have studied theoretically the factors influencing the ring strain in the series of heterocyclic α -lactones [41]. They suggested that replacement of the ring oxygen atom by sulphur would result in a marked decrease in the ring strain energy. According to this prediction, the α -carbonyl stretch-

ing frequency should be much lower in the sulphur containing heterocycles than in their oxygen analogues. Indeed, as mentioned above, for the five-membered heterocycles investigated in the present study the lowering of the carbonyl stretching frequency in going from the oxygen to the sulphur containing compound corresponds to 79.5 cm^{-1} . A similar situation was observed for the analogous six-membered α -lactones (see Scheme 2): matrix-isolated α -pyrone absorbs at 1757 cm^{-1} [33], while the thiapyran-2-one absorption shifts down to 1672 cm^{-1} [34]. It is worth noticing that the carbonyl frequency shift resulting from the ring $\text{O} \rightarrow \text{S}$ substitution (*ca.* 80 cm^{-1}) is more pronounced than the shift resulting from the ring size increase ($35\text{--}40\text{ cm}^{-1}$; see Table 4).

An increase of ring size may also be understood as an increase of the valence angles between adjacent bonds in the ring. If the heterocyclic lactones are idealized as regular polygons, then ring angles should vary as 60° , 90° , 108° and 120° on going from triangle to hexagon, and the latter should be considered as strain-free. These idealized values are quite close to the values of the valence $\text{C}\text{--}\text{C}(\text{O})\text{--}\text{C}$ angle found for the cycloalkanone rings of the corresponding size [42]. It is then interesting to analyze the values of the $\text{X}\text{--}\text{C}\text{--}\text{C}$ angles in the title compounds, where the vertex corresponds to the carbonyl carbon atom and X stands for the ring heteroatom. The calculated values for the $\text{O}\text{--}\text{C}(\text{O})\text{--}\text{C}$ angle in furanone amount to *ca.* 107.5° (Table 4) and increase by *ca.* 1.5° for the $\text{S}\text{--}\text{C}(\text{O})\text{--}\text{C}$ angle in thiophenone, thus confirming that the local ring strain around the carbonyl group is smaller when the ring contains sulphur as heteroatom. The same trend is observed for the six-membered heterocycles, α -pyrone and thiapyran-2-one, where the $\text{X}\text{--}\text{C}\text{--}\text{C}$ angle increases by *ca.* 2° with the $\text{O} \rightarrow \text{S}$ substitution, being *ca.* 117° in thiapyran-2-one (see Table 4).



Scheme 2. Six-membered heterocyclic α -carbonyl compounds, α -pyrone (AP) and thiapyran-2-one (TP), analogous to 2(5H)-furanone and 2(5H)-thiophenone. In order to keep the atom numbering consistent between five- and six-membered rings, the carbonyl oxygen was left without number.

Table 4

Selected spectral and geometric parameters calculated at the B3LYP/6-311++G(d,p) and MP2/6-311++G(d,p) levels of theory for 2(5H)-furanone (X=O), 2(5H)-thiophenone (X=S), α -pyrone (AP, X=O), and thiapyran-2-one (TP, X=S) monomers (see Schemes 1 and 2 for atom numbering)

Parameter ^a	Furanone	Thiophenone	AP	TP
Frequency				
C=O stretch exp	1793.5	1713.9	1757.0	1672.0
C=O stretch DFT	1841.3	1778.5	1817.6	1741.6
C=O stretch MP2	1837.9	1748.9	1812.1	1713.1
Angle				
X–C–C angle (DFT)	107.3	108.6	114.7	116.6
X–C–C angle (MP2)	107.6	109.1	115.1	117.2
Bond length				
C2=O (DFT)	119.8	120.2	120.1	121.0
C2–C3 (DFT)	148.4	148.1	145.0	145.0
C3=C4 (DFT)	133.2	133.3	135.7	136.1
C4–C5 (DFT)	149.9	149.9	143.1	143.0
C5=C6 (DFT)			135.0	135.4
C2=O (MP2)	120.4	121.2	120.8	122.2
C2–C3 (MP2)	148.6	148.4	145.5	145.3
C3=C4 (MP2)	134.0	134.2	136.3	137.0
C4–C5 (MP2)	150.1	150.2	143.3	142.8
C5=C6 (MP2)			135.7	136.6

^a Frequencies in cm^{-1} , angles in degrees, bond lengths in pm.

The present structural data may also shed some light on the conjugation effects in the α -carbonyl heterocycles. The calculated CC bond lengths (Table 4), for the formally single and double bonds, differ by 15–16 pm in the five-membered rings, while the same difference in the six-membered rings amounts to 7–8 pm only. This indicates that the conjugation effects are much stronger in the six-membered compounds. The reduction in the conjugation in the five-membered rings also reflects itself in the bond lengths of the attached carbonyl groups, which are systematically calculated to be shorter in furanone and thiophenone than in AP and TP (Table 4). Furthermore, in agreement with the calculations, the C=C stretching frequencies are observed at *ca.* 1611 cm^{-1} in furanone (Table 2) and 1615 cm^{-1} in thiophenone (Table 3), while in the six-membered compounds, the half-sums of the two C=C stretching frequencies fall at *ca.* 1595 and 1576 cm^{-1} [33,34].

4.3. Natural bond orbitals (NBO) analysis

NBO analysis provides an electronic structure description akin to the classic Lewis bonding theory [43–46]. Filled NBOs, empty bond NBOs and non-Lewis extra valence Rydberg orbitals, as well as their interactions according to second order perturbation theory analysis of the Fock matrix [43], are considered in this analysis. In

Table 5

Optimized geometric parameters^a and natural atomic charges of 2(5H)-furanone and 2(5H)-thiophenone calculated at the B3LYP/6-311++G(d,p) and MP2/6-311++G(d,p) levels of theory^b

	2(5H)-Furanone		2(5H)-Thiophenone	
	B3LYP	MP2	B3LYP	MP2
Bond length				
X1–C2	137.9	137.6	182.5	179.7
C2–C3	148.4	148.6	148.1	148.4
C3=C4	133.2	134.0	133.3	134.2
C4–C5	149.9	150.1	149.9	150.2
C5–X1	143.1	142.9	182.9	181.1
C2=O6	119.8	120.4	120.2	121.2
C3–H7	107.9	108.1	108.2	108.4
C4–H8	108.2	108.4	108.4	108.6
C5–H9	109.5	109.5	109.4	109.4
C5–H10	109.5	109.5	109.4	109.4
Angle				
C5–X1–C2	109.8	109.7	92.4	93.0
X1–C2–C3	107.3	107.6	108.6	109.1
C2–C3=C4	108.8	108.6	115.3	114.6
C3=C4–C5	109.0	108.6	116.7	116.0
C4–C5–X1	105.0	105.4	107.0	107.3
X1–C2=O6	122.6	122.8	123.8	124.2
C2–C3–H7	122.1	122.3	118.8	119.3
C3=C4–H8	127.8	127.9	123.9	124.2
C4–C5–H9	112.7	112.3	111.2	110.4
C4–C5–H10	112.7	112.3	111.2	110.4
Dihedral angle				
C3=C4–C5–H9	118.4	118.2	119.9	120.0
C3=C4–C5–H10	–118.4	–118.2	–119.9	–120.0
Charge/e				
X1	–0.547	–0.631	0.204	0.199
C2	0.758	0.921	0.376	0.496
C3	–0.297	–0.322	–0.289	–0.312
C4	–0.148	–0.112	–0.116	–0.077
C5	–0.061	0.018	–0.544	–0.508
O6	–0.555	–0.655	–0.540	–0.641
H7	0.230	0.223	0.230	0.222
H8	0.216	0.207	0.214	0.203
H9	0.202	0.175	0.232	0.209
H10	0.202	0.175	0.232	0.209

^a X1=O for furanone, X1=S for thiophenone. Dihedral angles are shown only for the two hydrogen atoms situated outside of the symmetry plane. Bond lengths in pm, angles and dihedral angles in degrees.

^b See atom numbering in Scheme 1.

Table 6
Selected natural bond orbitals of 2(5H)-furanone obtained from the MP2/6-311++G(d,p) calculations^a

Bond orbital ^b <i>T(A–B)</i>	Occupancy ^c (<i>e</i>)	Coefficients (%)		Description
		<i>A</i>	<i>B</i>	
$\sigma(\text{O1–C2})$	1.99288	69.68	30.32	$\sigma_{(\text{O1–C2})} = 0.8347\text{sp}^{(2.28)} + 0.5507\text{sp}^{(2.78)}\text{d}^{(0.02)}$
$\sigma(\text{O1–C5})$	1.99003	68.72	31.28	$\sigma_{(\text{O1–C5})} = 0.8290\text{sp}^{(2.44)} + 0.5593\text{sp}^{(3.86)}\text{d}^{(0.03)}$
$\sigma(\text{C2–C3})$	1.98186	48.60	51.40	$\sigma_{(\text{C2–C3})} = 0.6972\text{sp}^{(1.65)} + 0.7169\text{sp}^{(2.45)}\text{d}^{(0.01)}$
$\sigma(\text{C2=O6})$	1.99651	35.07	64.93	$\sigma_{(\text{C2=O6})} = 0.5922\text{sp}^{(1.80)}\text{d}^{(0.01)} + 0.8058\text{sp}^{(1.39)}$
$\pi(\text{C2=O6})$	1.98857	27.20	72.80	$\pi_{(\text{C2=O6})} = 0.5215\text{pd}^{(0.01)} + 0.8532\text{p}$
$\sigma(\text{C3=C4})$	1.98537	50.04	49.96	$\sigma_{(\text{C3=C4})} = 0.7074\text{sp}^{(1.66)}\text{d}^{(0.01)} + 0.7069\text{sp}^{(1.67)}$
$\pi(\text{C3=C4})$	1.91147	54.01	45.99	$\pi_{(\text{C3=C4})} = 0.7349\text{p} + 0.6782\text{p}$
$\sigma(\text{C4=C5})$	1.98398	50.23	49.77	$\sigma_{(\text{C4=C5})} = 0.7087\text{sp}^{(2.33)} + 0.7055\text{sp}^{(2.34)}\text{d}^{(0.01)}$
$\sigma(\text{C3–H7})$	1.98481	61.27	38.73	$\sigma_{(\text{C3–H7})} = 0.7827\text{sp}^{(2.00)} + 0.6224\text{s}$
$\sigma(\text{C4–H8})$	1.98673	60.46	39.54	$\sigma_{(\text{C4–H8})} = 0.7775\text{sp}^{(2.07)} + 0.6288\text{s}$
$\sigma(\text{C5–H9})$	1.97787	58.97	41.03	$\sigma_{(\text{C5–H9})} = 0.7679\text{sp}^{(3.01)}\text{d}^{(0.01)} + 0.6405\text{s}$
$\sigma(\text{C5–H10})$	1.97787	58.97	41.03	$\sigma_{(\text{C5–H10})} = 0.7679\text{sp}^{(3.01)}\text{d}^{(0.01)} + 0.6405\text{s}$
$n_1(\text{O1})$	1.97417			$n_1(\text{O1}) = \text{sp}^{(1.47)}$
$n_2(\text{O1})$	1.86348			$n_2(\text{O1}) = \text{p}$
$n_1(\text{O6})$	1.97986			$n_1(\text{O6}) = \text{sp}^{(0.72)}$
$n_2(\text{O6})$	1.87256			$n_2(\text{O6}) = \text{pd}^{(0.04)}$
$\text{Ry}_1(\text{C2})$	0.01556			$\text{Ry}_1(\text{C2}) = \text{sp}^{(5.82)}\text{d}^{(0.06)}$
$\text{Ry}_2(\text{C2})$	0.01047			$\text{Ry}_2(\text{C2}) = \text{pd}^{(1.22)}$
$\sigma^*(\text{O1–C2})$	0.08544	30.32	69.68	$\sigma^*_{(\text{O1–C2})} = 0.5507\text{sp}^{(2.28)} - 0.8347\text{sp}^{(2.78)}\text{d}^{(0.02)}$
$\sigma^*(\text{O1–C5})$	0.01006	31.28	68.72	$\sigma^*_{(\text{O1–C5})} = 0.5593\text{sp}^{(2.44)} - 0.8290\text{sp}^{(3.86)}\text{d}^{(0.03)}$
$\sigma^*(\text{C2–C3})$	0.05569	51.40	48.60	$\sigma^*_{(\text{C2–C3})} = 0.7169\text{sp}^{(1.65)} - 0.6972\text{sp}^{(2.45)}\text{d}^{(0.01)}$
$\sigma^*(\text{C2=O6})$	0.01041	64.93	35.07	$\sigma^*_{(\text{C2=O6})} = 0.8058\text{sp}^{(1.80)}\text{d}^{(0.01)} - 0.5922\text{sp}^{(1.39)}$
$\pi^*(\text{C2=O6})$	0.18272	72.80	27.20	$\pi^*_{(\text{C2=O6})} = 0.8532\text{pd}^{(0.01)} - 0.5215\text{p}$
$\sigma^*(\text{C3=C4})$	0.00884	49.96	50.04	$\sigma^*_{(\text{C3=C4})} = 0.7069\text{sp}^{(1.66)}\text{d}^{(0.01)} - 0.7074\text{sp}^{(1.67)}$
$\pi^*(\text{C3=C4})$	0.03780	45.99	54.01	$\pi^*_{(\text{C3=C4})} = 0.6782\text{p} - 0.7349\text{p}$
$\sigma^*(\text{C4=C5})$	0.01532	49.77	50.23	$\sigma^*_{(\text{C4=C5})} = 0.7055\text{sp}^{(2.33)} - 0.7087\text{sp}^{(2.34)}\text{d}^{(0.01)}$
$\sigma^*(\text{C3–H7})$	0.01102	38.73	61.27	$\sigma^*_{(\text{C3–H7})} = 0.6224\text{sp}^{(2.00)} - 0.7827\text{s}$
$\sigma^*(\text{C4–H8})$	0.01142	39.54	60.46	$\sigma^*_{(\text{C4–H8})} = 0.6288\text{sp}^{(2.07)} - 0.7775\text{s}$
$\sigma^*(\text{C5–H9})$	0.01916	41.03	58.97	$\sigma^*_{(\text{C5–H9})} = 0.6405\text{sp}^{(3.01)}\text{d}^{(0.01)} - 0.7679\text{s}$
$\sigma^*(\text{C5–H10})$	0.01916	41.03	58.97	$\sigma^*_{(\text{C5–H10})} = 0.6405\text{sp}^{(3.01)}\text{d}^{(0.01)} - 0.7679\text{s}$

The *A* and *B* values correspond to the contributions of the atomic orbitals of the two atoms forming a bond (by order of appearance in the corresponding entry in the first column) for the NBO orbitals extracted from the polarization coefficients [43] given in the description of the NBO orbitals.

^a The presented description is made in the space of the input atomic orbitals [as given by the 6-311++G(d,p) basis set used in the calculations].

^b See atom numbering in Scheme 1.

^c Occupancy is given with an exaggerated accuracy, as in the Gaussian output file.

the NBO analysis presented below, the calculated MP2/6-311++G(d,p) wavefunctions were considered.

The NBO charges [43] calculated for furanone and thiophenone are shown in Table 5. The striking difference between the two compounds is in the charge of the heteroatom: *ca.* $-0.6 e$ for oxygen (furanone) and $+0.2 e$ for sulphur (thiophenone). In furanone, due to the most electronegative ring heteroatom, (i) C2 and C5 are considerably more positive than in thiophenone, (ii) the carbonyl bond is more polarized and (iii) the methylene hydrogen atoms are less positive. These results support the interpretation given above regarding the frequency down-shift of the methylene stretching and bending vibrations in going from furanone to thiophenone. On the other hand, as discussed previously in detail for simpler molecules [47,48], the electronic structure of the $\text{C}=\text{C}(\text{=O})\text{--X}$ ($\text{X}=\text{O}, \text{S}$) fragments and the specific effects due to the $\text{O} \rightarrow \text{S}$ substitution are too much complex to be elucidated taking into account only the charges on atoms.

The selected NBOs, that were calculated to have a significant occupancy, are presented in Tables 6 and 7 for furanone and thiophenone, respectively. The description is made in the space of input atomic orbitals [as given by the 6-311++G(d,p) basis set used in the calculations]. The tables also show the percentage ratio of the atomic orbitals on each atom forming a bond, for the NBO orbitals extracted from the polarization coefficients [43]. The NBO analysis supports the idea of a greater polarization of the C–H methylenic bonds in thiophenone (*ca.* 59%:41%, see Table 7) when compared with furanone (*ca.* 61%:39%, see Table 6). The greater polarization of the ring X–C bonds in furanone (69%:31% average) than in thiophenone (48%:52% average) is also evident from Tables 6 and 7 and corresponds well to the difference in the atomic charges (Table 5).

Regarding the carbonyl bond in the two molecules studied, the NBO analysis reveals the following features: (i) the $\sigma(\text{C}=\text{O})$ bonding orbital is, as expected, strongly polarized towards the oxygen atom, the occupancy being slightly larger for thiophenone (1.998 *e*, vs. 1.997 *e* in furanone), (ii) the $\pi(\text{C}=\text{O})$ bonding orbital is even more polarized towards the oxygen atom, but in this case the occupancy is larger for furanone (1.989 *e*, vs. 1.988 *e* in thiophenone), (iii) the $\sigma^*(\text{C}=\text{O})$ and $\pi^*(\text{C}=\text{O})$ anti-bonding orbitals are polarized towards the carbon atom, the first showing a larger occupancy in furanone and the second in thiophenone; the occupancy of the $\pi^*(\text{C}=\text{O})$ anti-bonding orbitals in both molecules is considerably large (0.183 and 0.197 *e*, in furanone and thiophenone, respectively), (iv) in both molecules the carbonyl carbon atom is, as expected, hybridized sp^2 , with the two hybrid orbitals forming the σ bond with the carbonyl oxygen and C3 having a larger *s* character and the one connecting C2 to the ring heteroatom having an increased *p* character, (v) also in the two molecules, the carbonyl oxygen atom is hybridized *sp*, with one of the two hybrid orbitals forming the $\sigma(\text{C}=\text{O})$ bond and the other being occupied by a lone-pair of electrons; the two *p* orbitals form the $\pi(\text{C}=\text{O})$ bond and accommodate the second lone electron pair, (vi) the occupancy of the *sp*-hybrid lone-pair orbital of the carbonyl oxygen is relatively high in the two molecules (1.980 and 1.977 *e*, in furanone and thiophenone, respectively), while that of the second lone-pair orbital is considerably low (1.873 and 1.877 *e*, in furanone and thiophenone, respectively), indicating that the latter orbital is extensively involved in charge donation.

Taking into account occupancies of the $\sigma(\text{C}=\text{O})$ and $\pi(\text{C}=\text{O})$ orbitals in the two molecules and those of the corresponding $\sigma^*(\text{C}=\text{O})$ and $\pi^*(\text{C}=\text{O})$ anti-bonding orbitals, the relative strength of the carbonyl bond in furanone and thiophenone can be esti-

Table 7
Selected natural bond orbitals of 2(5H)-thiophenone obtained from the MP2/6-311++G(d,p) calculations^a

Bond orbital ^b T(A–B)	Occupancy ^c (e)	Coefficients (%)		Description
		A	B	
$\sigma(S1-C2)$	1.97874	49.47	50.53	$\sigma(S1-C2) = 0.7034sp^{(4.84)}d^{(0.05)} + 0.7108sp^{(2.65)}d^{(0.01)}$
$\sigma(S1-C5)$	1.98249	46.66	53.34	$\sigma(S1-C5) = 0.6831sp^{(5.04)}d^{(0.04)} + 0.7303sp^{(3.54)}d^{(0.02)}$
$\sigma(C2-C3)$	1.98277	49.26	50.74	$\sigma(C2-C3) = 0.7019sp^{(1.60)} + 0.7123sp^{(2.32)}d^{(0.01)}$
$\sigma(C2=O6)$	1.99790	34.53	65.47	$\sigma(C2=O6) = 0.5876sp^{(1.90)}d^{(0.01)} + 0.8092sp^{(1.29)}$
$\pi(C2=O6)$	1.98792	29.23	70.77	$\pi(C2=O6) = 0.5406pd^{(0.01)} + 0.8413p$
$\sigma(C3=C4)$	1.98617	50.25	49.75	$\sigma(C3=C4) = 0.7088sp^{(1.62)} + 0.7054sp^{(1.63)}$
$\pi(C3=C4)$	1.90393	54.15	45.85	$\pi(C3=C4) = 0.7358p + 0.6772p$
$\sigma(C4-C5)$	1.98512	49.00	51.00	$\sigma(C4-C5) = 0.7000sp^{(2.20)} + 0.7142sp^{(2.34)}d^{(0.01)}$
$\sigma(C3-H7)$	1.97930	61.20	38.80	$\sigma(C3-H7) = 0.7823sp^{(2.14)}d^{(0.01)} + 0.6229s$
$\sigma(C4-H8)$	1.98214	60.27	39.73	$\sigma(C4-H8) = 0.7764sp^{(2.25)}d^{(0.01)} + 0.6303s$
$\sigma(C5-H9)$	1.97874	60.73	39.27	$\sigma(C5-H9) = 0.7793sp^{(3.14)}d^{(0.01)} + 0.6267s$
$\sigma(C5-H10)$	1.97874	60.73	39.27	$\sigma(C5-H10) = 0.7793sp^{(3.14)}d^{(0.01)} + 0.6267s$
$n_1(S1)$	1.98765			$n_1(S1) = sp^{(0.49)}$
$n_2(S1)$	1.85205			$n_2(S1) = p$
$n_1(O6)$	1.97746			$n_1(O6) = sp^{(0.78)}$
$n_2(O6)$	1.87735			$n_2(O6) = p$
$Ry_1(C2)$	0.01764			$Ry_1(C2) = sp^{(5.09)}d^{(0.02)}$
$Ry_2(C2)$	0.00854			$Ry_2(C2) = sp^{(1.47)}d^{(4.57)}$
$\sigma^*(S1-C2)$	0.08985	50.53	49.47	$\sigma^*(S1-C2) = 0.7108sp^{(4.84)}d^{(0.05)} - 0.7034sp^{(2.65)}d^{(0.01)}$
$\sigma^*(S1-C5)$	0.01062	53.34	46.66	$\sigma^*(S1-C5) = 0.7303sp^{(5.04)}d^{(0.04)} - 0.6831sp^{(3.54)}d^{(0.02)}$
$\sigma^*(C2-C3)$	0.05365	50.74	49.26	$\sigma^*(C2-C3) = 0.7123sp^{(1.60)} - 0.7019sp^{(2.32)}d^{(0.01)}$
$\sigma^*(C2=O6)$	0.00845	65.47	34.53	$\sigma^*(C2=O6) = 0.8092sp^{(1.90)}d^{(0.01)} - 0.5876sp^{(1.29)}$
$\pi^*(C2=O6)$	0.19714	70.77	29.23	$\pi^*(C2=O6) = 0.8413pd^{(0.01)} - 0.5406p$
$\sigma^*(C3=C4)$	0.01026	49.75	50.25	$\sigma^*(C3=C4) = 0.7054sp^{(1.62)} - 0.7088sp^{(1.63)}$
$\pi^*(C3=C4)$	0.03985	45.85	54.15	$\pi^*(C3=C4) = 0.6772p - 0.7358p$
$\sigma^*(C4-C5)$	0.01444	51.00	49.00	$\sigma^*(C4-C5) = 0.7142sp^{(2.20)} - 0.7000sp^{(2.34)}d^{(0.01)}$
$\sigma^*(C3-H7)$	0.01314	38.80	61.20	$\sigma^*(C3-H7) = 0.6229sp^{(2.14)}d^{(0.01)} - 0.7823s$
$\sigma^*(C4-H8)$	0.01343	39.73	60.27	$\sigma^*(C4-H8) = 0.6303sp^{(2.25)}d^{(0.01)} - 0.7764s$
$\sigma^*(C5-H9)$	0.01929	39.27	60.73	$\sigma^*(C5-H9) = 0.6267sp^{(3.14)}d^{(0.01)} - 0.7793s$
$\sigma^*(C5-H10)$	0.01929	39.27	60.73	$\sigma^*(C5-H10) = 0.6267sp^{(3.14)}d^{(0.01)} - 0.7793s$

The A and B values correspond to the contributions of the atomic orbitals of the two atoms forming a bond (by order of appearance in the corresponding entry in the first column) for the NBO orbitals extracted from the polarization coefficients [43] given in the description of the NBO orbitals.

^a The presented description is made in the space of the input atomic orbitals [as given by the 6-311++G(d,p) basis set used in the calculations].

^b See atom numbering in Scheme 1.

^c Occupancy is given with an exaggerated accuracy, as in the Gaussian output file.

Table 8
Stabilization energies for the selected orbital pairs as given by the second order perturbation theory analysis of Fock matrix in NBO basis for 2(5H)-furanone and 2(5H)-thiophenone obtained from the MP2/6-311++G(d,p) calculations^a

Pair name	Donor NBO	Acceptor NBO	2(5H)-Furanone $E(2)^b$	2(5H)-Thiophenone $E(2)^b$
A	$\pi(C3=C4)$	$\pi^*(C2=O6)$	28.56	29.25
B	$n_2(X1)$	$\pi^*(C2=O6)$	51.24	39.51
C	$n_1(O6)$	$Ry_1(C2)$	22.88	22.57
D	$n_2(O6)$	$\sigma^*(X1-C2)$	45.57	41.78
E	$n_2(O6)$	$\sigma^*(C2-C3)$	24.19	23.18

^a See atom numbering in Scheme 1.

^b Energies in kcal mol⁻¹.

mated. A good descriptor of the bond strength is obtained by subtracting the occupancies of the anti-bonding orbitals from those associated with the corresponding bonding orbitals. The result of this operation for σ and π carbonyl bonds gives 1.986 and 1.806 e for furanone, while for thiophenone these occupancies are 1.989 and 1.793 e. These results indicate that the σ component of the carbonyl bond is slightly stronger in thiophenone than in furanone, but the π component is considerably stronger in furanone. The total ($\sigma + \pi$) occupancies amount to 3.792 and 3.782 e, in furanone and thiophenone, respectively. Hence, these results demonstrate that the carbonyl bond is stronger in furanone and justify the higher frequency observed for the carbonyl stretching vibration in furanone comparing with thiophenone.

The C5–X–C2 linkages were also found to present some interesting characteristics. According to the NBO results, in furanone the ring oxygen atom is hybridized sp², with the two hybrid orbi-

tals involved in the C5–O and C2–O bonds exhibiting a strong polarization towards the oxygen atom and having an increased p character. In turn, the third hybrid orbital, which corresponds to a lone-electron pair (lp) orbital, has a reduced p character (see Table 6). The second lone-electron pair orbital exhibits pure p character, which favours the π delocalization within the O=C–O fragment. The hybridization of sulphur in thiophenone is also essentially of sp² type, but with large distortions relative to the standard s–p characters of the hybrid orbitals. As for furanone, one lp orbital in thiophenone exhibits pure p character favoring the π delocalization within the O=C–S fragment. The second lp orbital is a hybrid orbital with high s character (ca. 67%; see Table 7), whereas the remaining two hybrid orbitals, which are involved in the C5–S and C2–S bonds, possess high p character (over 82% each). From the occupancy of the orbitals associated with the C5–X and C2–X bonds (see Tables 6 and 7), it can also be concluded that these bonds are considerably stronger in furanone than in thiophenone, which is easy to rationalize in terms of better overlap between the atomic orbitals of the O and C atoms (belonging to the same row of the periodic table) when compared with those of S and C. This also allows to conclude, in good agreement with previously obtained data for simpler molecules containing the O=C–O or O=C–S groups [47,48], that the mesomerism within the O=C–O fragment in furanone is more important than that within the O=C–S moiety in thiophenone.

Table 8 shows the results of the second order perturbation theory analysis of Fock matrix in NBO basis. This analysis is carried out by examining all possible stabilizing interactions between “filled” (donor) Lewis-type NBOs and “empty” (acceptor) non-Lewis NBOs, and estimating their energetic importance by the 2nd-order

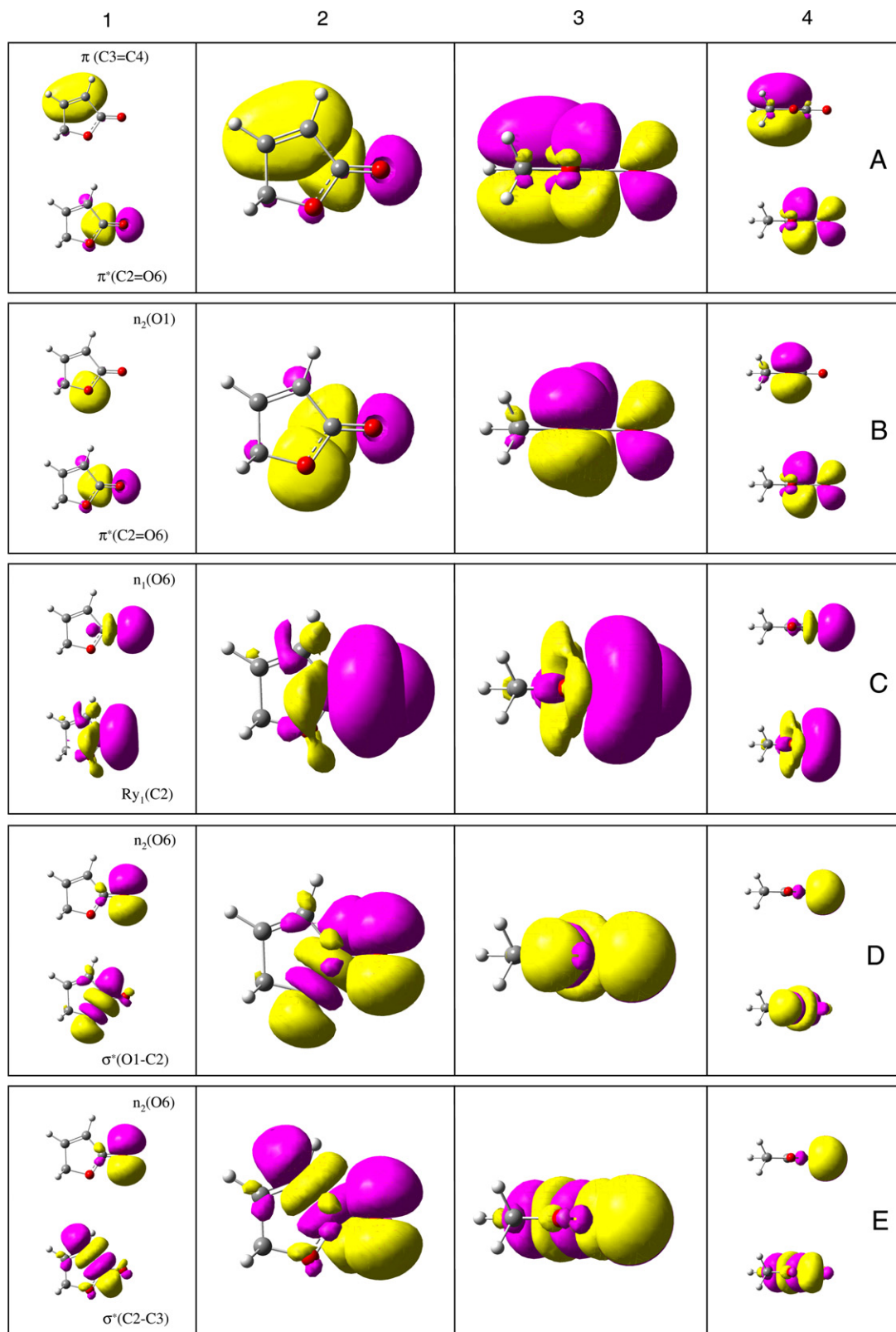


Fig. 4. Electron density surfaces of selected pre-orthogonalized NBOs of 2(5H)-furanone calculated at the MP2/6-311++G(d,p) level. Yellow and pink colors correspond to opposite signs. Isovalues of the electron densities are equal to 0.02 e. The rows named as A, B, C, D, E correspond to the orbital pairs with the same names in Table 8. All particular orbitals are denominated in Column 1, which also displays the front views of the donor NBOs and acceptor NBOs (separate for each orbital); Column 2: front views of the donor and acceptor NBOs (superimposed); Column 3: side views of the donor and acceptor NBOs (superimposed); Column 4: side views of the donor NBOs and acceptor NBOs (separate). The frontmost portions of the orbitals in cells A1, A2, B1 and B2 are removed for clarity. The removed portions have opposite sign and are symmetric to the lobes displayed in the cells A1–B2 (compare to cells A3–B4, where the entire orbitals are displayed). Color codes for atoms: red, oxygen; grey, carbon; white, hydrogen. (For interpretation of the references in colour in this figure legend, the reader is referred to the web version of this article.)

perturbation theory [43]. Since these interactions lead to donation of occupancy from the localized NBOs of the idealized Lewis structure into the empty non-Lewis orbitals (and thus, to departures from the idealized Lewis structure description), they are sometimes also referred to as “delocalization” corrections to the zeroth-order natural Lewis structure. For each donor NBO (i) and acceptor NBO (j), the stabilization energy $E(2)$ associated with delocalization $i \rightarrow j$ is estimated as

$$E(2) = \Delta E_{ij} = q_i \frac{F(i,j)^2}{\varepsilon_j - \varepsilon_i}$$

where q_i is the donor orbital occupancy, ε_i , ε_j are diagonal elements (orbital energies) and $F(i,j)$ is the off-diagonal NBO Fock matrix element. In Table 8 only the most important interactions (corresponding to the largest $E(2)$ values) are presented. These interactions are also illustrated graphically in Fig. 4 for the case of furanone (as discussed in detail below and shown in Table 8, in thiophenone the orbital interactions are analogous).

The energetically most relevant interactions in both studied molecules are the following: (i) charge transfer from the p-type lone-electron pair of the ring heteroatom to the $\pi^*(\text{C}=\text{O})$ orbital (Fig. 4B), which is a measure of the delocalization within the $\text{O}=\text{C}-\text{X}$ fragment. This interaction (pair B in Table 8), as expected, is considerably more important for furanone than for thiophenone ($E(2) = 51.24$ vs. 39.51 kcal mol $^{-1}$); (ii) charge transfer from the in-plane p-type lone-electron pair of the carbonyl oxygen to the $\sigma^*(\text{C}2-\text{X})$ anti-bonding orbital (pair D in Table 8; see also Fig. 4D). This interaction is nearly as important in furanone as in thiophenone; (iii) interaction (pair E) between the in-plane p-type lp orbital of the carbonyl oxygen and the $\sigma^*(\text{C}2-\text{C}3)$ orbital (Fig. 4E) is also similar in both compounds and is complementary to the previous pair; (iv) the $\pi(\text{C}3=\text{C}4) \rightarrow \pi^*(\text{C}=\text{O})$ interaction (pair A) correlates with the π -electron delocalization within the $\text{C}4=\text{C}3-\text{C}2=\text{O}$ fragment, and is equal in the two studied molecules; (v) finally, the NBO analysis also indicates the existence of a significant back-donation effect involving the sp-hybrid lone-electron pair orbital of the carbonyl oxygen and the carbonyl carbon atom, through a Rydberg orbital of the latter (pair C).

An important conclusion that can be extracted from this analysis is that all the most representative NBO interactions (except pair B) are nearly energetically equal in the two studied compounds (Table 8). Thus, charge transfer from the p-type lone-electron pair of the ring heteroatom to the $\pi^*(\text{C}=\text{O})$ orbital (which accounts for the delocalization within the $\text{O}=\text{C}-\text{X}$ fragment) is the important interaction (pair B, Table 8) making distinction in the physicochemical behaviour of the two molecules, including ring strain and thermal and photochemistry. In spectroscopic terms, this might also be related with the most striking difference found in the spectra of the two compounds, i.e., the considerably frequency decrease of the carbonyl stretching vibration in going from furanone to thiophenone.

5. Conclusion

The experimental FTIR spectra of the monomers of 2(5H)-furanone and 2(5H)-thiophenone isolated in low temperature argon matrices are reported for the first time. The experimental infrared data were assigned with the help of theoretical calculations of the vibrational spectra carried out at the MP2 and DFT levels of theory with the 6-311++G(d,p) basis set and subsequent normal-coordinate analyses. Natural Bond Orbital (NBO) analyses carried out for the two studied compounds revealed important details of their electronic structure and shed light on the most important intramolecular interactions, also providing a way for the establishment of important spectra-structure correlations. Additional correlations

were obtained from comparison between the two title compounds and their six-membered ring analogues, α -pyrone and thiapyran-2-one.

Acknowledgements

This work was funded by Fundação para a Ciência e a Tecnologia (FCT), Grant #SFRH/BD/16119/2004 and Projects POCI/QUI/59019/2004 and POCI/QUI/58937/2004, also supported by FEDER.

Appendix A. Supplementary data

Table S1 contains optimized structures of 2(5H)-furanone, 2(5H)-thiophenone, α -pyrone and thiapyran-2-one and the corresponding Cartesian coordinates obtained at the DFT/B3LYP and MP2 theory levels using the 6-311++G(d,p) basis set. Supplementary data associated with this article can be found, in the online version, at doi:10.1016/j.molstruc.2008.02.034.

References

- [1] D. Martinelli, G. Grossmann, U. Sequin, H. Brandl, R. Bachofen, BMC Microbiology 4 (2004).
- [2] T.A. Mansoor, J. Hong, C.O. Lee, C.J. Sim, K.S. Im, D.S. Lee, J.H. Jung, J. Nat. Prod. 67 (2004) 721–724.
- [3] E.L. Ghisalberti, J.R. Hargreaves, E. McConville, Nat. Prod. Res. 18 (2004) 105–109.
- [4] B.S. Min, S.Y. Lee, J.H. Kim, O.K. Kwon, B.Y. Park, R.B. An, J.K. Lee, H.I. Moon, T.J. Kim, Y.H. Kim, H. Joung, H.K. Lee, J. Nat. Prod. 66 (2003) 1388–1390.
- [5] K.W. Cho, H.S. Lee, J.R. Rho, T.S. Kim, S.J. Mo, J. Shin, J. Nat. Prod. 64 (2001) 664–667.
- [6] R. Ratnayake, V. Karunaratne, B.M.R. Bandara, V. Kumar, J.K. MacLeod, P. Simmonds, J. Nat. Prod. 64 (2001) 376–378.
- [7] M. Ndagijimana, M. Vallicelli, P.S. Cocconcelli, F. Cappa, F. Patrignani, R. Lanciotti, M.E. Guerzoni, Appl. Environ. Microbiol. 72 (2006) 6053–6061.
- [8] K. Berryman, A.A. Doherty, J.M. Edmunds, W.J. Patt, M.C. Plummer, J.T.S. Repine, Substituted 2(5H)furanone, 2(5H)thiophenone and 2(5H)pyrrolone derivatives, their preparation and their use as endothelin antagonists, in: World Intellectual Property Organization, Warner-Lambert Company, 1995.
- [9] S.J. Cho, Bull. Korean Chem. Soc. 24 (2003) 731–732.
- [10] D.M. Boalino, J.D. Connolly, S. McLean, W.F. Reynolds, W.F. Tinto, Phytochemistry 64 (2003) 1303–1307.
- [11] M.V.N. De Souza, Mini-Rev. Org. Chem. 2 (2005) 139–145.
- [12] J.D. Coyle, Chem. Rev. 78 (1978) 97–123.
- [13] Y.S. Rao, Chem. Rev. 76 (1976) 625–694.
- [14] N.B. Carter, A.E. Nadany, J.B. Sweeney, J. Chem. Soc. Perkin Trans. 1 (2002) 2324–2342.
- [15] R. Alibés, A. Alvaréz-Larena, P. March, M. Figueiredo, J. Font, T. Parella, A. Rustullet, Org. Lett. 8 (2006) 491–494.
- [16] J. Gawronski, Q.H. Chen, Z. Geng, B. Huang, M.R. Martin, A.I. Mateo, M. Brzostowska, U. Rychlewska, B.L. Feringa, Chirality 9 (1997) 537–544.
- [17] T. Hjelmggaard, T. Persson, T.B. Rasmussen, M. Givskov, J. Nielsen, Bioorg. Med. Chem. 11 (2003) 3261–3271.
- [18] S. Latypov, X. Franck, J.C. Jullian, R. Hocquemiller, B. Figadere, Chem. Eur. J. 8 (2002) 5662–5666.
- [19] A.C. Legon, Chem. Rev. 80 (1980) 231–262.
- [20] A.C. Legon, J. Chem. Soc. Chem. Commun. (1970) 838.
- [21] J.L. Alonso, A.C. Legon, J. Chem. Soc. Faraday Trans. 2 77 (1981) 2191–2201.
- [22] A.G. Lesarri, J.C. López, J.L. Alonso, J. Mol. Struct. 273 (1992) 123–131.
- [23] W. Dianxun, W. Dong, L. Sheng, L. Ying, J. Electron Spectrosc. 70 (1994) 167–172.
- [24] W.S. Chin, Z.P. Xu, C.Y. Mok, H.H. Huang, H. Mutoh, S. Masuda, J. Electron Spectrosc. 88–91 (1998) 97–101.
- [25] A.A. Al-Saadi, J. Laane, J. Phys. Chem. A 111 (2007) 3302–3305.
- [26] A.D. Becke, Phys. Rev. A 38 (1988) 3098–3100.
- [27] C.T. Lee, W.T. Yang, R.G. Parr, Phys. Rev. B 37 (1988) 785–789.
- [28] S.H. Vosko, L. Wilk, M. Nusair, Can. J. Phys. 58 (1980) 1200–1211.
- [29] J.H. Schahtschneider, F.S. Mortimer, Vibrational Analysis of Polyatomic Molecules. VI. FORTRAN IV Programs for Solving the Vibrational Secular Equation and for the Least-Squares Refinement of Force Constants, Project No. 31450, Structural Interpretation of Spectra, Shell Development Co., Emeryville, CA, 1969.
- [30] M.J. Frisch, G.W. Trucks, H.B. Schlegel, G.E. Scuseria, M.A. Robb, J.R. Cheeseman, J.A. Montgomery, Jr., T. Vreven, K.N. Kudin, J.C. Burant, J.M. Millam, S.S. Iyengar, J. Tomasi, V. Barone, B. Mennucci, M. Cossi, G. Scalmani, N. Rega, G.A. Petersson, H. Nakatsuji, M. Hada, M. Ehara, K. Toyota, R. Fukuda, J. Hasegawa, M. Ishida, T. Nakajima, Y. Honda, O. Kitao, H. Nakai, M. Klene, X. Li, J.E. Knox,

- H.P. Hratchian, J.B. Cross, V. Bakken, C. Adamo, J. Jaramillo, R. Gomperts, R.E. Stratmann, O. Yazyev, A.J. Austin, R. Cammi, C. Pomelli, J.W. Ochterski, P.Y. Ayala, K. Morokuma, G.A. Voth, P. Salvador, J.J. Dannenberg, V.G. Zakrzewski, S. Dapprich, A.D. Daniels, M.C. Strain, O. Farkas, D.K. Malick, A.D. Rabuck, K. Raghavachari, J.B. Foresman, J.V. Ortiz, Q. Cui, A.G. Baboul, S. Clifford, J. Cioslowski, B.B. Stefanov, G. Liu, A. Liashenko, P. Piskorz, I. Komaromi, R.L. Martin, D.J. Fox, T. Keith, M.A. Al-Laham, C.Y. Peng, A. Nanayakkara, M. Challacombe, P.M.W. Gill, B. Johnson, W. Chen, M.W. Wong, C. Gonzalez, J.A. Pople, Gaussian 03, Revision C.02, Gaussian, Inc., Wallingford, CT, 2004.
- [31] R.J.D. Smith, R.N. Jones, *Can. J. Chem.* 37 (1959) 2092–2094.
- [32] R.N. Jones, C.L. Angell, T. Ito, R.J.D. Smith, *Can. J. Chem.* 37 (1959) 2007–2022.
- [33] S. Breda, I. Reva, L. Lapinski, R. Fausto, *Phys. Chem. Chem. Phys.* 6 (2004) 929–937.
- [34] I. Reva, S. Breda, T. Roseiro, E. Eusébio, R. Fausto, *J. Org. Chem.* 70 (2005) 7701–7710.
- [35] S. Breda, L. Lapinski, I. Reva, R. Fausto, *J. Photochem. Photobiol. A Chem.* 162 (2004) 139–151.
- [36] S. Breda, L. Lapinski, R. Fausto, M.J. Nowak, *Phys. Chem. Chem. Phys.* 5 (2003) 4527–4532.
- [37] N. Kus, S. Breda, I. Reva, E. Tasal, C. Ogretir, R. Fausto, *Photochem. Photobiol.* 83 (2007) 1237–1253; Erratum 83 (2007) 1541–1542.
- [38] A.Yu. Ivanov, A.M. Plokhhotnichenko, E.D. Radchenko, G.G. Sheina, Yu.P. Blagoi, *J. Mol. Struct.* 372 (1995) 91–100.
- [39] R.A. Nyquist, H.A. Fouchea, G.A. Hoffman, D.L. Hasha, *Appl. Spectrosc.* 45 (1991) 860–867.
- [40] W.J.M. van Tilborg, *Tetrahedron Lett.* (1973) 523–526.
- [41] R.D. Bach, O. Dmitrenko, *J. Am. Chem. Soc.* 128 (2006) 4598–4611.
- [42] R.J. Berry, R.J. Waltman, J. Pacansky, A.T. Hagler, *J. Phys. Chem.* 99 (1995) 10511–10520.
- [43] F. Weinhold, C.R. Landis, *Valency and Bonding. A Natural Bond Orbital Donor-Acceptor Perspective*, Cambridge University Press, New York, 2005.
- [44] F. Weinhold, C.R. Landis, *Chem. Educ. Res. Practice Eur.* 2 (2001) 91–104.
- [45] A.E. Reed, L.A. Curtiss, F. Weinhold, *Chem. Rev.* 88 (1988) 899–926.
- [46] J.P. Foster, F. Weinhold, *J. Am. Chem. Soc.* 102 (1980) 7211–7218.
- [47] R. Fausto, L.A.E. Batista de Carvalho, J.J.C. Teixeira-Dias, M.N. Ramos, *J. Chem. Soc. Faraday Trans. 2* 85 (1989) 1945–1962.
- [48] R. Fausto, *Theochem J. Mol. Struct.* 315 (1994) 123–136.